

Critical review of analytical models for the in-plane and out-of-plane assessment of URM buildings

S. Cattari, S. Lagomarsino, A. Bazzurro & F. Porta

*Department of Civil, Chemical and Environmental Engineering,
University of Genova, Italy*

S. Pampanin

*Department of Civil and Natural Resources Engineering, University of
Canterbury, Christchurch*



2015 NZSEE
Conference

ABSTRACT: The seismic assessment of URM buildings requires proper methods of analysis and verification procedures, which consider both out-of-plane and in-plane behavior within the ambit of the displacement-based approach. In addition to numerical models, which are able to analyze also complex structures, analytical mechanically-based models can be derived from standards and are effective to support risk mitigation policies. The facade of a two-storey URM building has been considered as simple case study, and the results in terms of %NBS provided by different standards of methods from literature are compared. Regarding the out-of-plane behavior, some possible collapse mechanisms have been considered, in order to check the different methods of evaluation of the displacement demand and definition of the ultimate capacity. For the in-plane behavior, first of all a discussion on the different failure criteria for piers and spandrels is presented, and then the response of one single pier and the adjacent spandrels is investigated, in order to check the mutual interaction. Some comments on critical issues in present standards and proposals for a new release of NZSEE are also presented.

1 INTRODUCTION

The Canterbury earthquake sequence in 2010-2011 testified once again the high vulnerability of URM buildings. Therefore, proper methods of analysis and verification procedures are necessary to support risk mitigation policies, which are proposed both for current existing building in international standards and even for cultural heritage masonry structures (Lagomarsino and Cattari 2015). Together with the detailed assessment provided by numerical models, also the use of analytical models based on a limited number of mechanical and geometrical parameters is very useful in order to provide a first evaluation of the expected performance (e.g. based on %NBS as proposed in NZSEE 2006) and indicate whether and to what extent a more refined approach is necessary.

Within this context and according to the displacement-based approach the paper presents a comparison among some different models proposed in national and international codes/standards (NZSEE 2006, Eurocode 8-part 3 2005, ASCE 41-13 2014, Italian Building Code 2008, named in the following as NZSEE, EC8-3, ASCE and NTC respectively) with regard to the analysis of both the in-plane and out-of-plane response of URM buildings. The differences and analogies among the different formulations are critically discussed with the support of a reference case study building consisting of a two-storey brick masonry structure.

While for the out-of-plane response the comparison includes both the basis of seismic analysis and the criteria of verification, in the case of in-plane response it is limited, for the sake of simplicity, to the response of single panels (piers and spandrels), that constitutes the basis for the consequent assessment of entire wall/building. However, it is worth noting that also in this latter case, codes present some differences in the evaluation of the demand (by overdamped, as in NZSEE and ASCE, or inelastic spectra, as in EC8-3 and NTC).

2 REFERENCE CASE STUDY

Figure 1 illustrates the case study building adopted as a reference for the comparison of alternative assessment methods, which consists of a two-storey brick masonry wall with good mortar joints. The mechanical parameters herein adopted (as summarized in Table 1) correspond to a medium brick and mortar hardness and are in accordance with the recent results of in-situ experimental campaigns performed in New Zealand after the Canterbury earthquake sequence in 2010-2011 (Giaretton et al. 2014), which also form the basis reference values adopted for the revised version of NZSEE2006 Assessment guidelines (currently being finalized and from here on referred to as NZSEE-r).

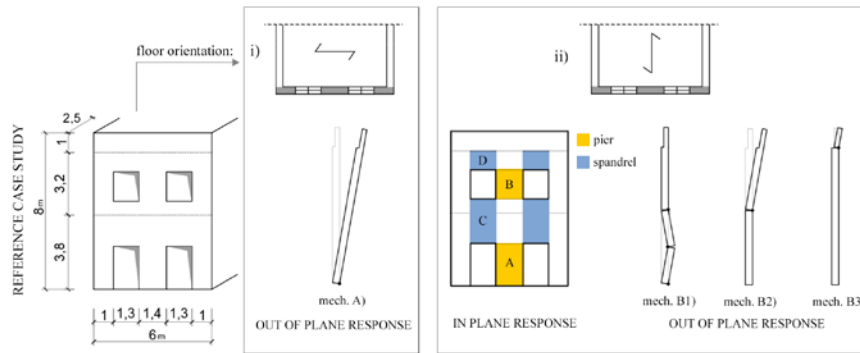


Figure 1. Reference Case Study building and mechanisms considered depending on floor orientation.

Table 1. Geometrical data and mechanical parameters adopted for the reference case study building.

	Geometrical data [m]					Mechanical parameters [MPa]	Value
	h_p	l_p	t_p	λ_p	σ_{INF}/f_m	(Names and symbols adopted by codes)	
Pier A	2.2	1.4	0.36	1.57	0.023	Masonry compressive strength (f_d, f_c, f_m)	10.6
Pier B	1.5	1.4	0.36	1.07	0.01	Local cohesion of mortar joints (c, f_{vm0}, v_{be})	0.5
	h_{sp}	l_{sp}	t_{sp}	λ_{sp}		Local friction coefficient of mortar joints (μ)	0.6
Spandrel C	1.3	2.3	0.36	1.3		Conventional tensile strength of masonry (f_{dt}, f_t)	0.41
Spandrel D	1.3	1	0.36	0.81		Tensile strength of blocks (f_{bt})	3.1
Parapet	1		0.23			Compressive strength of block (f'_b, f_{bk})	26

The response of the two-storey masonry wall is analyzed assuming two scenarios for the main orientation of the horizontal diaphragms (timber floor and roof, both with a total load equal to 1.5 kN/m² comprehensive of the permanent and accidental loads combined for the seismic assessment).

In the first scenario (i), the timber floor at the 1st level and the roof are supported by the lateral walls (and the connection between the façade and the lateral walls is neglected). In this case the assessment is only focused on the most dangerous mechanism that is the overturning of the whole façade, which is very slender assuming as the seismic input that at the ground level (Mech. A).

In the second scenario (ii), the timber floor at the 1st level is supported by the façade (with a tributary length equal to 2.5 m). In this case both the in-plane and out-of-plane responses should be assessed. For the out-of-plane response, the possible mechanisms are: B1) out-of-plane of the wall at the first storey spanning vertically (2 blocks mechanism); B2) overturning of the upper part of the façade, around a hinge at the first level; B3) overturning of the parapet. The seismic input of the type B mechanisms is increased, as a function of the elevation of the constraint with the rest of the building.

For the in-plane response, the attention is focused only on the assessment of shear supported by piers (named as A and B in Figure 1) and not on that of the entire wall. Through the elementary system illustrated in Figure 2, the effects of the interaction between the pier and the adjacent spandrels are taken into account. In particular, in order to estimate in a simple way the force-drift relationship (V- θ) of the pier, the following basic steps are performed: firstly (step I), the elastic prediction in terms of bending moments at the end sections (M_{up} and M_{inf}) is obtained from the resolution of the linear system; then (step II), the admissibility of the elastic solution of bending moment at up section is checked with respect the ultimate strength compatible with the criteria discussed in §4.1 and, if

necessary, corrected. To this aim, the final shear supported by the pier (V_u) is computed: firstly (step IIa), by evaluating the ultimate bending moment $M_{up,ul}$ compatible with that transferred by the adjacent spandrels ($M_{s,ul}$) and those reached at the end sections of the pier (by using the expressions for *Rocking/Crushing* failure mode illustrated in Table 2 as a function of the axial load acting on two end sections); then (step IIb), by checking the compatibility of the shear associated to the flexural mode with that of the shear failure mode (*Diagonal Cracking* and *Bed Joint Sliding*). Once computed the maximum strength of the pier, the evolution of the force-drift relationship depends on the prevailing mechanism previously checked. In particular, if the bending moment $M_{up,ul}$ is limited by that of the spandrels, as a function of the response of these latter (if brittle or ductile), the capacity curve may develop in a different way (Figure 2). Finally, it is evident that such correction procedure may alter also the position of the contraflexural point in the pier (from $h_{0,el}$ to $h_{0,mod}$ as illustrated in Figure 2).

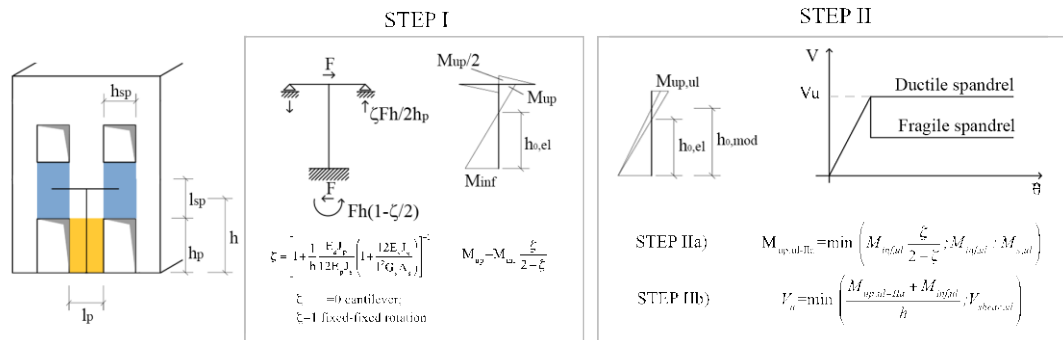


Figure 2. Pier-Spandrel Interaction: equivalent system and analytical model proposed.

3 ASSESSMENT OF MASONRY ELEMENTS UNDER OUT-OF-PLANE ACTIONS

3.1 Theoretical Background and motivations for a Displacement-Based Approach

The behavior of masonry elements under out-of-plane seismic actions is mainly related to geometric stability rather than to the strength of materials. Due to the negligible tensile strength of masonry and the slenderness of masonry walls, particularly when insufficiently connected to orthogonal walls and horizontal diaphragms, these elements can lose static equilibrium for very low values of Peak Ground Acceleration (PGA). However, damage observation after strong seismic events, as well as shaking table tests, have proved that dynamic equilibrium is still possible after the rocking mechanism has been activated. Therefore, there is a need of assessment procedures, even at the level of engineering practice, to take into account the dynamics of rocking mechanisms. As the use of nonlinear dynamic analysis would be too complicated (Housner 1963), a displacement-based approach (DBA) was proposed as a simplified method for the assessment of rocking masonry structures (Priestley and Evison 1978, Doherty et al. 2002, Lagomarsino 2015), in spite of some conceptual limitations (Makris and Konstantinidis 2003).

Limit analysis, under the theoretical framework of plasticity theory for masonry structures (Heyman 1966), can be applied via either the static theorem, which provides a lower-bound or safe solution, and/or the kinematic theorem, which provides an upper-bound of the load multiplier of inertial masses, after assuming a collapse mechanism for a given masonry element, defined by its geometry and all inertial masses and applied forces.

In this paper we will consider two different recurring mechanisms: a) vertical cantilever (Mech. B2 and B3 in Figure 1); b) wall spanning vertically between two horizontal diaphragms (Mech. B2 in Figure 1). The system is subjected to permanent actions and to horizontal inertial actions, proportional to masses through a seismic multiplier. The static multiplier α_0 that induces the onset of rocking is obtained by evaluating the work done by equilibrated forces on a set of compatible generalized virtual displacements (Theorem of Virtual Works). Within the Force-Based Approach (FBA), this multiplier can be put in relation with the PGA, in the case of rigid blocks, or to the spectral acceleration $S_a(T)$, if a reference period of vibration of the element is assumed. DBA requires evaluating the seismic

multiplier α under an incremental kinematic analysis, that is by increasing step-by-step the rotation of blocks till to the condition of loss of static equilibrium. The obtained curve (horizontal multiplier versus displacement of a control point) is a sort of pushover curve, which can be transformed into capacity curve (spectral acceleration versus displacement) of the substitute structure (nonlinear equivalent Single Degree of Freedom System, SDOF), through formulations analogous to the one adopted for the pushover analysis of buildings.

The use of DBA, instead of the more traditional FBA, is by now adopted by different international standards (Sorrentino et al. 2015), including the NZSEE2006 guidelines on assessment of existing buildings (2006), currently under revision. Four verification procedures, based on the DBA, are compared herein for the assessment of the main façade of the case study building: 1) NZSEE (2006); 2) the draft document of the new/revised NZSEE-r (under preparation); 3) the Italian code NTC (2008); 4) an updated release of this procedure (Lagomarsino 2015, referred to as MB-perpetuate).

3.2 Selection of Load Pattern according to different approaches

The first difference between the NZSEE method, which is based on Doherty et al. (2002), and the Italian NTC, coherent with Lagomarsino (2015), is in the selection of the load pattern. Even if both methods are based on the same formulation for the substitute structure (Fajfar 1999), NZSEE assumes a linear displacement profile (coherent with the hypothesis of rigid blocks) and considers masses as distributed in the block, while NTC makes the simplification to concentrate all masses in each block in the corresponding barycenter. If a single block (vertical cantilever) is considered, in the case of NZSEE the participant mass is $\frac{3}{4}M$ (where M is the mass of the block) and the displacement of the substitute structure is that of the point at $\frac{2}{3}H$ (where H is the height of the block), while for NTC the equivalent s.d.o.f. system has mass M and displacement of the point at the center of the panel ($\frac{1}{2}H$). The outcome is that the two capacity curves are homothetic, being the one of NTC simplified by cautionary (in this case the application to complex multi-blocks collapse mechanisms is much simpler). Figure 3 shows the two capacity curves for a single block of thickness t .

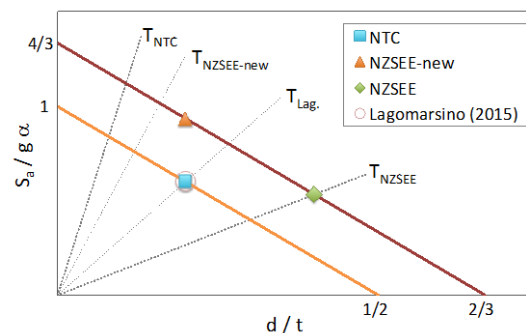


Figure 3. Capacity curves of a single block, ultimate displacement and secant periods, according to the four considered methods.

3.3 Evaluation of displacement Capacity and Demand

The further step of the DBA is to define the ultimate displacement capacity d_U . Both methods consider a fraction of the displacement d_0 for which the loss of static equilibrium occurs (Figure 3): 1) NZSEE - $d_U=0.6d_0$; 2) NZSEE-r - $d_U=0.3d_0$; 3) NTC - $d_U=0.4d_0$; 4) MB-perpetuate - $d_U=0.4d_0$. The ultimate displacement represents a cautionary displacement for which the dynamic instability under rocking does not occur, unless for very few cases (low fractile considering many real records, in order take into account the record-to-record variability).

The last step is the evaluation of the displacement demand, which requires the definition of the reference period and the seismic input spectrum. For the first aspect, both NZSEE and Lagomarsino consider the classic Capacity Spectrum Method (Freeman 1998), which means to assume a linear equivalent s.d.o.f. with period $T_0 = 2\pi\sqrt{d_0/\alpha_0}$, while the other two methods adopt a secant period T_s , by considering a displacement d_s which is a fraction of d_U . ($0.8d_U$ in NZSEE-new; $0.4d_U$ in NTC).

Figure 3 shows the periods adopted by the four methods.

Regarding the seismic input all methods, except MB-perpetuate, consider the elastic spectrum at 5% of viscous damping. Differently, MB-perpetuate adopts an overdamped spectrum, based on the observation that a slight increase of dissipation occurs in masonry walls under rocking, as they are not really rigid blocks. Moreover, difference among methods can be observed in the amplification of motion due to filtering effect of the main building (floor spectrum). NZSEE and NZSEE-r propose a homothetic amplification of the spectrum, through a proper coefficient related to the position of the mechanism in the building, while NTC and MB-perpetuate define a more accurate floor spectrum, which is amplified around the fundamental period of the building.

It is worth noting the definition of the capacity curve is not explicitly stated in NZSEE, but it can be directly derived from the provided information: i) displacement d_0 ; ii) ultimate (d_U, T_U) and secant (d_S, T_S) displacements and periods (the second ones given by empirical formulas), which allows to evaluate the corresponding spectral accelerations (S_{a_U}, S_{a_S}).

All methods take into account the limited compressive strength of masonry, by a reduced effective thickness, that is related to the stress block in NTC or defined by an empirical formula in NZSEE.

In the case of a wall spanning vertically between two horizontal constraints, the definition of the spectral displacement is made through the participation factor γ . The formula proposed by NZSEE provides very low values (even lower than 1) and seems to be theoretically inconsistent, as it depends also on the vertical load applied at the top.

3.4 Comparison of predicted performance of the case study building

In the following the results obtained by the application of such procedures for the reference case study examined are illustrated. The assessment has been made by considering the spectral shape as per NZS1170.5 (2004) with a seismic coefficient of $Z=0.22$, corresponding to the “traditional” seismic input for Christchurch before the occurrence of the Canterbury earthquake sequence in 2010-2011 and a soil class C. The %NBS was evaluated for the four mechanisms (A, B1, B2 and B3) by the four different methods (Table 2).

Table 2. Assessment of the considered collapse mechanisms by the four methods, in terms of %NBS.

%NBS	A (whole façade)	B1 (2 blocks)	B2 (upper façade)	B3 (parapet)
NZSEE	81	244	50	50
NZSEE-r	58	410	54	59
NTC	81	305	123	71
MB-perpetuate	54	222	70	87

Figure 4a shows the assessment of the overturning of the whole façade (mechanism A), with a comparison between the Acceleration Displacement Response Spectrum (ADRS) and the capacity curves defined by the different codes, which are homothetic in the linear descending branch; the initial elastic part of the curves is defined by assuming $T_e=0.4$ s for the NZSEE guidelines (both 2006 and revised version) and by considering the wall as an elastic cantilever for the other curve. Lagomarsino (2015) method considers, after activation of rocking ($T=2\pi\sqrt{d/S_a} > T_e$), an overdamped demand spectrum (damping reduction factor $\eta = \sqrt{10/(5+\xi)}$) by assuming the following equivalent viscous damping:

$$\xi = 0.05 - \xi_h \left[1 - (T_e/T)^\kappa \right] \quad (1)$$

where ξ_h is the maximum area-based hysteretic damping ($\xi_h=0.1$ in this case) and κ is a calibrated coefficient, usually ranging between 1 and 2. The relation is similar to the one proposed by Blandon and Priestley (2005), but uses T instead of the ductility μ to account for the effect of strength

degradation.

In order to compare the results obtained by the four methods, the ultimate displacement capacities and the corresponding seismic demands are indicated. Dotted lines show the secant periods used for the evaluation of the seismic demand.

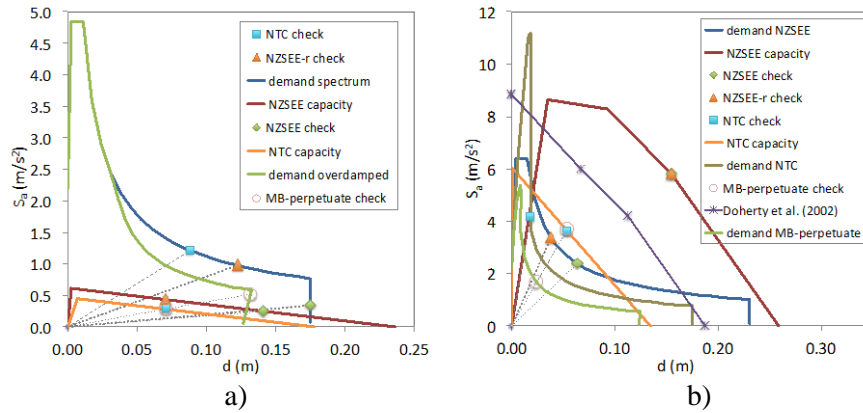


Figure 4. Displacement demands and capacities by the four methods: a) mechanism A; b) mechanism B1.

The %NBS obtained from the four methods vary between 54% to 81% (Table 2), which is a reasonable spread when considering the differences in the methods in terms of evaluation of ultimate displacement and the seismic demand. The PGA that activates the mechanism, evaluated by a FBA, ranges from 0.35 m/s^2 (NZSEE) to 0.43 m/s^2 (NTC); this confirms there is a big safety margin between activation and overturning (from 2.8 to 5.1).

Figure 4b shows the results for mechanism B1, consisting of the collapse of the first storey façade with the formation of two blocks. It is worth noting that NZSEE assumes the horizontal crack exactly at the center of the panel, while in NTC and MB-perpetuate it would be necessary to find the correct position, corresponding to the minimum value of the horizontal static multiplier (in this case at 0.59 of the interstorey height). As already mentioned, NZSEE formulation gives a participation factor $\gamma=1.09$, from which the capacity turns to be higher than what proposed by Doherty et al. (2002) which assumes $\gamma=1.5$. The %NBS is greater than 200 for all the methods (Table 2) indicating that the seismic input for Christchurch expected at 500 years design (PGA or $Z=0.3 \text{ g}$) is not even sufficient to trigger this specific mechanism B1. A MCE record, corresponding to 250 years return period and $R=1.8$ (spectral ordinate multiplier) could come closer from Figure 4b it is evident that the seismic demand spectra intersect the capacity curves in the elastic segment. For mechanisms of this type the FBA turns out to be usually sufficient for the assessment.

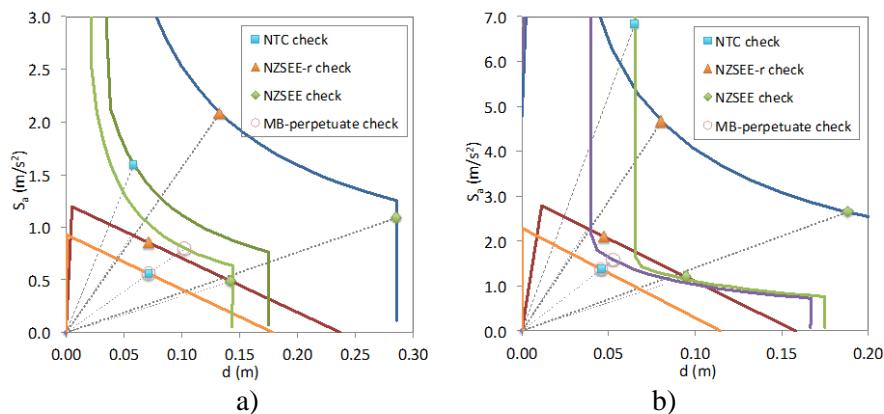


Figure 5. Assessment of mechanisms B2 (upper part of the façade) and B3 (parapet).

Figure 5a, which is zoomed on the capacity curves, shows results for the mechanism B2, corresponding to the overturning of the upper part of the façade as a vertical cantilever. If the comparison was made with the whole façade (mechanism A), the horizontal multiplier would be

higher due to the lower slenderness, but the seismic demand would be amplified by the response of the building; therefore, the %NBS would be comparable in the two cases. For mechanism B3 (Figure 5b), corresponding to the rocking and overturning of the parapet, the slenderness is even lower, but the seismic demand is further increased (because the element is at the top of the façade) and the displacement capacity is lower, because of the smaller thickness. The %NBS is again comparable to the previous mechanisms of vertical cantilever (e.g. B2 and A).

4 ASSESSMENT OF MASONRY ELEMENTS UNDER IN-PLANE RESPONSE

As far as the in-plane response of masonry panels is concerned, all the aforementioned codes refer to the adoption of strength criteria, based on mechanical or phenomenological hypotheses (Calvi and Magenes 1997, Calderini et al. 2009), aimed to capture the key failure modes, namely: *Rocking*, *Toe Crushing*, *Diagonal Shear Cracking* or *Bed Joint Sliding*. The failure domain of the panel is defined through the minimum value as predicted from all the considered failure criteria aimed to interpret such failure modes. Despite this common approach, various differences arise in the specific coefficients adopted, the meaning of mechanical parameters adopted and the failure criteria considered. Another important aspect is related to the criteria proposed to differentiate the behaviour of piers and spandrels: in the last decade various experimental campaigns highlighted the relevance of this issue (e.g. Beyer and Dazio 2012, Graziotti et al. 2012), and new formulations are under considerations for implementation in the new release of various codes (including the revised version of the NZSEE 2006).

4.1 Analytical models for piers

Table 3 summarizes the strength criteria for in-plane response proposed in the various codes herein considered for piers as a function of the aforementioned failure modes, together with a sketch aimed to clarify the cracking pattern that characterizes each of them and the critical point/section assumed as reference for their mechanical interpretation.

Regarding the flexural/bending response, two different failure modes are considered: *Rocking* and *Toe Crushing*. In both cases, the analytical models proposed in the international codes are based on the beam theory, neglecting the tensile strength of the material and assuming an appropriate normal stress distribution at the compressed toe. Indeed, the occurrence of one or the other failure mode depends only on the entity of the axial load acting on the pier; in fact, apart from ASCE, other codes do not differentiate the *Rocking* mechanism from the *Toe-Crushing mechanism*. From the equilibrium of the panel it is possible to define the ultimate bending moment of the section and, then, the ultimate shear supported by the panel as a function of the shear span related to the contraflexural point that takes into account for its actual boundary conditions (NTC, EC8-3, NZSEE): only ASCE explicitly refers to the two conventional schemes of fixed-fixed rotation and cantilever. Regarding the normal stress distribution, all codes refer to a stress block distribution by adopting different values for the reduction coefficient of the compressive strength (0.85 in NTC and NZSEE, $1/1.15=0.87$ in EC8-3, and 0.7 in ASCE).

Regarding the shear response, two different failure modes are usually considered: the *Bed Joint Sliding* and the *Diagonal Cracking*. In principle, both failure modes can occur in a masonry panel as one would prevail depending on the compression stress level acting on the panel. Despite this, only some codes explicitly take into account both of them, while usually they are proposed as alternative.

In the case of *Diagonal Cracking* two types of failure criteria may be recognized in literature (see Calderini et al. 2009 for a review of their theoretical principles): models describing masonry as a composite material with regular pattern, with cracks developing along the bed and head mortar joints, as well as within/across the blocks (adopted by NZSEE according to some modifications proposed in Calvi and Magenes 1997); models describing masonry as an equivalent isotropic material, considering the development of cracks along the principal compression stress directions (adopted by NTC and ASCE). Both models refer to the contribution of the whole area of the transversal section at the middle of the panel, assumed as fully compressed. All codes introduce a corrective factor (named b , β or $(1+\alpha_v)$ in various codes) to account for the shear stress distribution at the centre of the panel and relate the peak value to the mean one. Despite this common approach, then different expressions are

proposed, which consider only the effect associated to the slenderness (NTC and ASCE) or also that of boundary condition (NZSEE) of the panel.

Table 3. Summary of strength criteria proposed in the examined codes for piers.

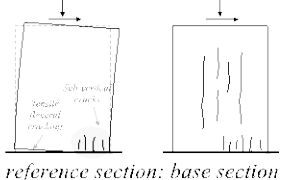
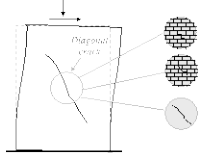
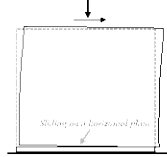
	 <p>Rocking / Toe Crushing reference section: base section</p>	 <p>Diagonal Cracking reference point: centre of the pier</p>	 <p>Bed Joint Sliding reference section: that with the shortest uncracked length</p>
NTC	$M = \frac{l^2 t \sigma_b}{2} \left(1 - \frac{\sigma_b}{0,85 f_d} \right)$	$V_i = \frac{l t f_c}{b} \sqrt{1 + \frac{\sigma}{f_c}}$ <p>Proposed as alternative to BIS only in case of existing masonry</p>	$V_t = l' t f_{vd}$ $\begin{cases} f_{vd} \leq \min(2,0 f_{bt}; 2,2 MPa) \\ f_{vd} = f_{m0} + 0,4 \sigma \end{cases}$
EC8-3	$V_f = \frac{Nl}{2h_0} (1 - 1,15 v_d)$	Not present	$V_t = l' t f_{vd}$ $\begin{cases} f_{vd} = f_{m0} + 0,4 \sigma \\ f_{vd} \leq 0,065 f_m \end{cases}$
NZSEE	$M_n = N \left(z - \frac{a}{2} \right) = N \left(z - \frac{1}{2} \cdot \frac{N}{0,85 f_t} \right)$	<p>through mortar joints:</p> $V_j = \frac{A(c' + \mu' \sigma)}{1 + \alpha}$ <p>through bricks</p> $V_b = \frac{A f_{bt}}{2,3(1 + \alpha)} \sqrt{1 + \frac{\sigma}{f_{bt}}}$	$V_s = \frac{3cz + \mu N}{1 + \frac{3acd}{N}}$
ASCE	<p>Toe Crushing:</p> $V_{tc} = (\alpha N + P_w) \frac{l}{h} \left(1 - \frac{\sigma}{0,7 f'_m} \right)$ <p>Rocking:</p> $V_r = 0,9(\alpha N + P_w) \frac{l}{h}$	$V_{dt} = f'_{dt} A \beta \sqrt{1 + \frac{\sigma}{f'_{dt}}}$	$V_{bis} = A v_{mc}$ $v_{mc} = 0,75 \cdot \frac{0,75 v_{lc} + \frac{N}{A}}{1,5}$
<p>Notes:</p> <ul style="list-style-type: none"> ✓ c' and μ' modified cohesion and friction coefficient ($c' = \frac{c}{1 + \mu \phi}$; $\mu' = \frac{\mu}{1 + \mu \phi}$) ✓ Coefficient aimed to account for the shear stress distribution at the centre of panel: <ul style="list-style-type: none"> ○ b (NTC): 1 for $\lambda < 1$; $b = \lambda$ for $1 < \lambda < 1,5$; 1,5 for $\lambda > 1,5$ ○ β (ASCE): 0,67 for $\lambda < 0,67$; $\beta = \lambda$ for $0,67 < \lambda < 1$; 1 for $\lambda > 1$ ○ $1 + \alpha$ (NZSEE): α is equal to h_{cr}/l and defines the position of the contraflexural point 			

Figure 6 compares the different values proposed in codes for such factor together with a new proposal of the Authors, derived from the results of parametrical nonlinear FEM analyses performed on panels characterized by different slenderness and boundary conditions (Cattari and Lagomarsino 2009, Calderini et al. 2009). The numerical results confirmed the influence also of the boundary conditions, although the expression assumed in NZSEE consistent with the original proposal of Calvi and Magenes 1997) leads to very conservative results, in particular for very squat panels (with slenderness lower than 0.5). Conversely, the expression assumed in NTC and ASCE provide in most cases (apart the fixed-fixed rotation condition) results on the unsafe side. On basis of these evidences, the following alternative is proposed assuming for the corrective factor b : 1 for $\lambda \leq 0,5$; $1 - 2\alpha$ for $\lambda \geq 1$ with a linear interpolation for intermediate values of the slenderness.

In the case of *Bed Joint Sliding*, usually a Mohr-Coulomb criterion is assumed as reference by

adopting the local values of cohesion and friction coefficient of mortar joints. However, while NTC, EC8-3 and NZSEE refer only to the compressed area of the wall, ASCE considers the whole cross section. In addition, in ASCE a coefficient equal to 1.5 is included to consider the actual shear stress distribution (thus with a meaning similar to the β coefficient introduced in case of the *Diagonal Cracking*, being 1.5 a reference value consistent with the beam theory in the case of a slender panel). As usually *Bed joint Sliding* occurs at the end sections (typically not entirely compressed at ULS), the adoption of the actual compressed area at the end sections seems to be more consistent, without the use of the coefficient 1.5. Moreover, codes further differ: in the conventional value assumed for the friction coefficient (0.4 in NTC and EC8-3 and 1 in ASCE, being related to the actual quality of mortar only in NZSEE); and in the limit value assumed for the masonry shear strength f_{vd} (as resulting from the application of the Mohr-Coulomb criterion) in order to take into account also the possible failure of blocks.

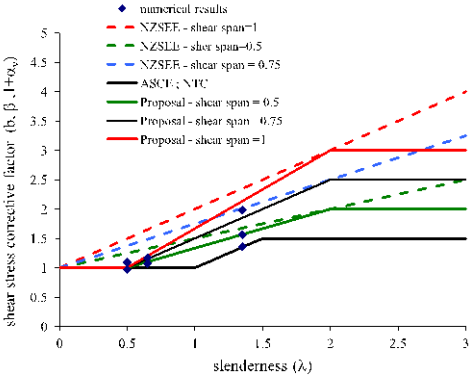


Figure 6. Comparison among the expression proposed by codes for corrective factor of shear stress.

As previously introduced, the strength domain of the panel is finally obtained as the minimum prediction provided by all criteria (and failure modes) considered by each code. Figure 7 illustrates the resulting Shear-Axial capacity domains for panels A, in the case of cantilever condition, and B, in the case of fixed-fixed rotation; two vertical lines refer to the compressive state of two given case studies. The domain named as “Proposal” refers to the following assumptions: for *Rocking/Toe Crushing* a criterion consistent with ASCE; for *Diagonal Cracking* with that of NZSEE by adopting the alternative coefficient proposed instead of $(1+\alpha_v)$; for *Bed Joint Sliding* with that of NTC and EC8-3 neglecting the limitation of shear strength on blocks. These assumptions are under discussion within the Committee for the revision of the NZSEE2006 document. A comparison also with experimental results that support some of such choices is illustrated in Calderini et al. (2009).

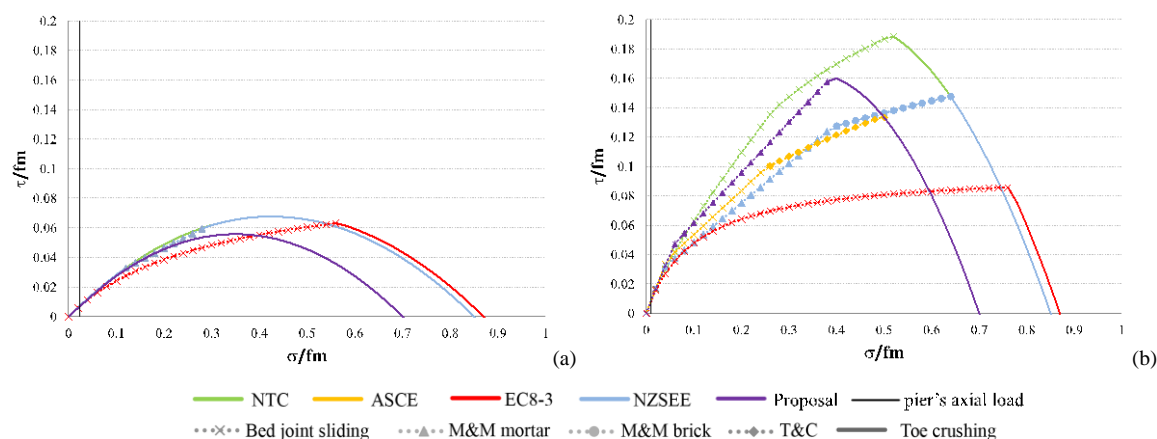


Figure 7. Strength domain of panels A (a) and B (b) of the examined case study.

From Figure 7, it is worth noting that:

- the panel is squat (B) and coupled to spandrels the more the shear failure modes may be significant for the response of the pier;
- for low values of the axial load ($\sigma < 0.05-0.1f_m$), when flexural behaviour tends to prevail, the differences in predictions of codes are negligible
- for moderate-high value of the axial load ($0.05-0.1f_m < \sigma < 0.4 f_m$), when shear may prevail, major differences can be noted, in some cases in the order of 100% or more. In the case of *Bed Joint Sliding*, the limitation of the joint failure provided by the failure of blocks is significant for increasing values of the axial load (being the limitation of EC8-3 very conservative);
- finally, in the region where *Crushing* prevails, the coefficient adopted for the stress block becomes very important. As panels are typically within the limit of $0.4f'_m$, such difference is not so relevant in the practice apart very few cases.
- more Analytical models for spandrels.

Failure criteria for spandrels have been addressed in literature and proposed only very recently, due to the general lack of experimental results able to support mechanical formulations. As a result very few specific criteria are proposed in codes, which usually assume the spandrel behaviour as that of a pier rotated by 90° (provided that an effective lintel/architrave is supporting the spandrel, as explicitly indicated in EC8-3, NTC, ASCE). Only NTC makes a distinction in the strength criterion to be adopted for spandrels as a function of the acting axial load (if known or unknown from the analysis) and ASCE points out the relevance of the issue indicating some literature references without explicitly adopting any of them.

Actually, spandrel behaviour differs from that of piers mainly for two reasons: i) the interlocking phenomena that may originate at the end section with the adjacent masonry portion; ii) the interaction with the architrave/lintel that in particular affects the residual strength, which is strongly dependent on the axial load acting on the spandrel. A comprehensive review of criteria proposed in literature for spandrels is illustrated in Beyer and Mangalathu (2013). Herein the attention is only focused on the interpretation of flexural behaviour, considered as one of the most critical issues as its inadequate prediction may significantly affects the interaction with piers, leading to a possibly significant underestimation of the actual capacity of the overall base shear of the masonry walls/buildings.

Spandrels, differently from piers, due to the interlocking phenomena aforementioned (see also Fig. 8a), may rely on the contribution of an “equivalent tensile strength” ($f_{t,sp}$) that alters the flexural strength domain discussed in §4.1 for piers, at least with reference to the peak strength. This is recognized by different proposals in literature (Cattari and Lagomarsino 2009, Beyer 2012, FEMA 306 1998) and also confirmed by some experimental evidences (Beyer and Mangalathu 2013).

Table 4 illustrates the expressions proposed for $f_{t,sp}$ and those consequent for the ultimate bending moment at peak and residual conditions. It is worth noting that in Beyer (2012) further additional terms are included to take into account also for the contribution provided by the lintel/architrave coupled to spandrel and the adoption of these criteria is under examination for the ongoing updating of NZSEE-new, being ahead to other codes on this issue.

Table 4. Summary of expressions proposed in literature for the equivalent tensile strength of spandrels.

	FEMA 306	Cattari and Lagomarsino 2009	Beyer 2012
$f_{t,sp}$	$f_{p,sj} = 0,5 (0,75c)$ $f_{p,bj} = 0,5(0,75c + \gamma_{sp} \sigma_p)$	$f_{tu} = \min(\mu \gamma_{sp} \sigma_p \frac{l_b}{2(h_j + h_b)}, \frac{f_{bt}}{2})$	$f_{bj} = (\mu \gamma_{sp} \sigma_p + c) \frac{l_b}{2(h_b + h_j)}$ $f_{hj} = \frac{c}{2\mu}; f_{t,sp} = f_{bj} + f_{hj}$
Peak strength	$M_{p,ft} = \frac{2}{3} l_s (f_{p,bj} t_b \frac{l_b}{2} + f_{p,sj} h_b \frac{l_b}{2} (NB - 1)) \frac{l_s}{4(h_j + h_b)}$	$M_N = f(N, \frac{f_{t,sp}}{f_{bm}}, \mu_c, \mu_t)$	$M_{p,ft} = (f_{t,sp} + \sigma_{sp}) \frac{h_{sp}^2 t_{sp}}{6}$
Residual strength	$M_{r,ft} = \frac{1}{2} l_s f_{r,bj} t_b (\frac{l_b}{2} - \Delta_s) \frac{l_s}{2(h_j + h_b)}$		$V_{r,ft} = \frac{\sigma_{sp} l_s}{h_s} (1 - \frac{\sigma_{sp}}{0,85 f_{bm}})$
Notes:	<ul style="list-style-type: none"> - h_b, l_b and h_j: height and length of blocks and height of mortar joints, respectively - γ_{sp}: coefficient aimed to take into account the amount of vertical stresses transferred by piers at end section of spandrels (equal to 0.5 in FEMA 306, 0.65 in Cattari and Lagomarsino 2008 and a function of slenderness of spandrel in Beyer 2012) - σ_{sp} and σ_p: axial stress acting on spandrel and adjacent pier, respectively 		

Figure 8b illustrates a comparison among the aforementioned proposals for the spandrel C of the reference case study by assuming a fixed-fixed rotation condition and neglecting the contribution of collar joint proposed in FEMA 306. In the examined case the contribution associated to the friction of horizontal mortar joints is almost negligible due to the very low axial load acting on the piers (approximately equal to $0.02f_m$). Accounting for the cohesive contribution of joints (even without that of the head ones) may result into a significant increase in strength. It seems reasonable that once cracked (i.e. when reaching the peak) the spandrel loses such contribution: it means that it suddenly drops to the residual strength, according to Cattari and Lagomarsino 2009 or, in a more conservative approach, Beyer 2012. The proposal of FEMA 306 appear more questionable because the effect of the axial load of spandrel is neglected and due to the symmetric distribution stress assumed that does not differentiate between compression and tension.

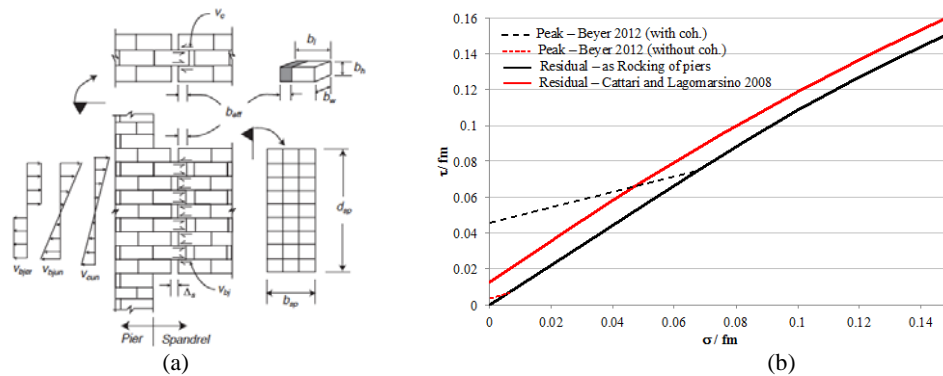


Figure 8. Contributions considered in FEMA 306 for the computation of equivalent tensile strength of spandrel (a) and flexural strength domain of spandrels according to literature proposals (b).

Even low (as usual for example for spandrels at top level) to consider the effect of equivalent tensile strength may produce relevant effects at scale of the whole walls/buildings and leads to damage more consistent with the observed one (Cattari and Lagomarsino 2009).

4.2 Interaction between piers and spandrels in the case study building

Figure 9 illustrates the pushover curves resulting for pier A that account also for the interaction with spandrels according to the simplified analytical formulation illustrated in §2. Moreover the most significant data that clarify the variation of the point of controflexure in the piers when moving from the elastic prediction to that which considers also the maximum admissible strength on various sections/elements are summarized in Figure 9. In the case of piers, due to the low acting axial load, the *Rocking* response is the dominant one: thus, there is not a significant difference among criteria proposed by codes as discussed in §4.1. In the case of spandrels, the strength has been computed according to the expression proposed in Beyer 2012 by considering or not the cohesive contribution either of head and bed joints. If this latter is considered effective, then the spandrel does not limit the bending moment on section UP: thus, it would be possible to rely on a ductile behaviour of pier and higher strength. Conversely, if neglected (because of the poor quality of joints or some pre-cracked condition), the spandrels affects the ultimate strength achievable on section UP (Fig.2): then, the evolution of pushover curve of the pier may differ as a function of the expected behaviour of spandrel (if brittle or ductile). Indeed, even in this second case, more precautionary, the beneficial effect on the strength of pier provided by the spandrel coupling mechanism results in an strength increase equal to 19% (pier A) and 9% (pier B) than the cantilever condition.

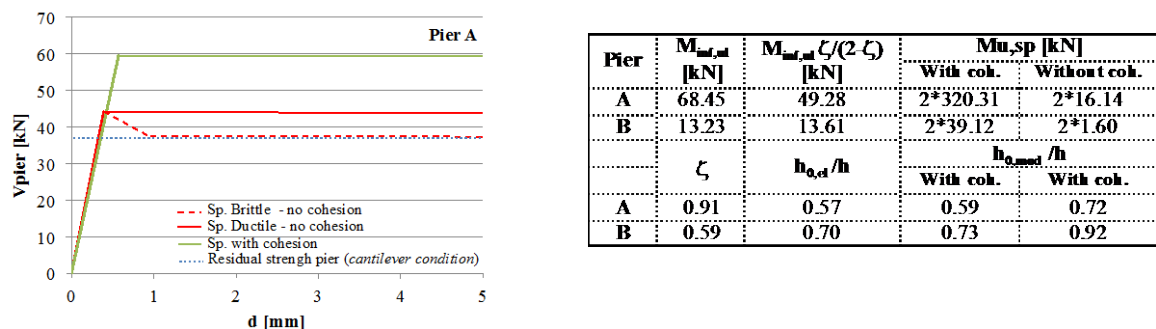


Figure 9. Pushover curves resulting from panel A and summary of results.

This application wants to be a simple example aimed to highlight the relevance of taking into account – even in a simplified way – the interaction between piers and spandrels. It represents a first step to assess the hierarchy of strength between these two elements and develop simple analytical tools based on analogous principles to those already adopted for other structural types (e.g. reinforced concrete as illustrated in Pampanin, 2006) useful for a simple but effective application of PBA.

5 ACKNOWLEDGMENTS

The authors acknowledge the financial contribution to the research provided by the EQC Project 14/660 “Vulnerability analysis of unreinforced masonry churches” (funded by the New Zealand Earthquake Commission, 2014) and the Italian Network of Seismic Laboratories (RELUIS), in the frame of the 2014 RELUIS III Project (Topic: Masonry Structures).

6 REFERENCES

- ASCE/SEI 41-13 (2014). Seismic Evaluation and Retrofit of Existing Buildings. American Society of Civil Engineers, Reston, VA, ISBN 978-0-7844-7791-5.
- ATC (1998). FEMA-306 Evaluation of earthquake damaged concrete and masonry wall buildings. Basic Procedures Manual, Applied Technology Council, Washington DC.
- Beyer, K. (2012) Peak and residual strengths of brick masonry spandrels, *Engineering Structures*, 41: 533-547.
- Beyer, K., Mangalathu, S. (2013). Review of strength models for masonry spandrels, *Bull Earth Eng*, 11:521–542.
- EN 1998-3 (2005) Eurocode 8: Design of structures for earthquake resistance - Part 3: Assessment and retrofitting of buildings. CEN (European Committee for Standardization), Brussels, Belgium.

- Calderini, C., S. Cattari & S. Lagomarsino (2009). In-plane strength of unreinforced masonry piers, *Earthq Eng Struct Dynam*, 38(2): 243-267.
- Cattari, S. and S. Lagomarsino (2008). *A strength criterion for the flexural behaviour of spandrel in unreinforced masonry walls*, Proceedings of the 14th WCEE, Beijing, China.
- Cattari, S., S. Lagomarsino (2009) *Modelling the seismic response of unreinforced existing masonry buildings: a critical review of some models proposed by codes*, Proc. of 11th Canadian Masonry Symposium, Toronto.
- NZSEE (2006). Assessment and improvement of the structural performance of buildings in earthquake. Recommendations of a NZSEE Study Group, New Zealand Society for Earthquake Engineering, Wellington, New Zealand (the updating process is ongoing).
- Lagomarsino, S. and S. Cattari. 2015. PERPETUATE guidelines for seismic performance-based assessment of cultural heritage masonry structures, *Bull Earth Eng*, 13(1), 13-47, DOI:10.1007/s10518-014-9674-1.
- NTC 2008 (2008) Decreto Ministeriale 14/1/2008. Norme tecniche per le costruzioni. Ministry of Infrastructures and Transportations. G.U. S.O. n.30 on 4/2/2008 (in Italian).
- Beyer, K. and A. Dazio (2012). Quasi-static monotonic and cyclic tests on composite spandrels, *Earthquake Spectra*, 28(3): 885-906.
- Blandon, C.A. and M.J.N. Priestley (2005). Equivalent viscous damping equations for direct displacement based design, *Journal of Earthquake Engineering*, 9(SI 2):257-278.
- Doherty, K., M.C. Griffith, N.T.K. Lam and J.L. Wilson (2002). Displacement-based analysis for out-of-plane bending of seismically loaded unreinforced masonry walls. *Earthq Eng Struct Dynam*, 31(4):833-850.
- Fajfar, P. (1999). Capacity spectrum method based on inelastic demand spectra, *Earthq Eng Struct Dynam*, 28(9):979-993.
- Freeman, S.A. (1998). *Development and use of capacity spectrum method*, Proceedings of the 6th U.S. National Conference on Earthquake Engineering, Seattle, CD-Rom, Paper #269, EERI, Oakland, Ca
- Giaretton, M., D.Dizhur, F. da Porto and J.M. Ingham (2014). *Unreinforced stone masonry buildings in New Zealand: Inventory, assessment and improvement*, Proceedings of the 9th IMC, Guimarães, July 7-9, 2014, Portugal.
- Graziotti, F., G. Magenes and A. Penna (2012). *Experimental cyclic behaviour of stone masonry spandrels*, Proceedings of the 15th WCEE, Lisbon, Portugal.
- Heyman, J. (1966). The stone skeleton, *International Journal of Solids and Structures*, 2:249-279
- Housner, G.W. (1963). The behavior of inverted pendulum structures during earthquakes, *Bull Seismol Soc Am*, 53:403-417.
- Lagomarsino, S. (2015). Seismic assessment of rocking masonry structures, *Bull Earth Eng*, 13(1): 97-28.
- Magenes, G. and G.M. Calvi (1997). In-plane seismic response of brick masonry walls, *Earthq Eng Struct Dynam*, 26: 1091-1112.
- Makris, N. and D. Konstantinidis (2003). The rocking spectrum and the limitations of practical design methodologies, *Earthq Eng Struct Dynam*, 32(2):265-289
- Pampanin, S. (2006). Controversial Aspects in Seismic Assessment and Retrofit of Structures in Modern Times: Understanding and Implementing Lessons from Ancient Heritage, *Bulletin of NZ Society of Earthquake Engineering*, June, Vol. 39, N.2, 120-133
- Priestley, M.J.N., R.J. Evison and A.J. Carr (1978). Seismic response of structures free to rock on their foundations, *Bull N Z Nat Soc Earthq Eng*, 11(3):141-150.
- Sorrentino, L., D. D'Ayala, G. de Felice, M.C. Griffith, S. Lagomarsino and G. Magenes. Review of out-of-plane SEISMIC assessment techniques applied to existing masonry buildings, *Int. J. Architectural Heritage* (submitted).